Published in final edited form as:
Dev Biol. 2007 August 1; 308(1): 30–43.

Drosophila dopamine synthesis pathway genes regulate tracheal morphogenesis

Anita Hsouna[a,1], **Hakeem O. Lawal**[b,1], **Iyare Izevbaye**[b,2], **Tien Hsu**[a,*], and **Janis M. O'Donnell**[a,*]

a*Department of Pathology and Laboratory Medicine, and Hollings Cancer Center, Medical University of South Carolina, Charleston, South Carolina 29425, USA*

b*Department of Biological Sciences, University of Alabama, Tuscaloosa, Alabama 35487, USA*

Abstract

While studying the developmental functions of the *Drosophila* dopamine synthesis pathway genes, we noted interesting and unexpected mutant phenotypes in the developing trachea, a tubule network that has been studied as a model for branching morphogenesis. Specifically, *Punch* (*Pu*) and *pale* (*ple*) mutants with reduced dopamine synthesis show ectopic/aberrant migration, while *Catecholamines up (Catsup)* mutants that over-express dopamine show a characteristic loss of migration phenotype. We also demonstrate expression of Punch, Ple, Catsup and dopamine in tracheal cells. The dopamine pathway mutant phenotypes can be reproduced by pharmacological treatments of dopamine and a pathway inhibitor 3-iodotyrosine (3-IT), implicating dopamine as a direct mediator of the regulatory function. Furthermore, we show that these mutants genetically interact with components of the endocytic pathway, namely *shibire/dynamin* and *awd/nm23*, that promote endocytosis of the chemotactic signaling receptor Btl/FGFR. Consistent with the genetic results, the surface and total cellular levels of a Btl-GFP fusion protein in the tracheal cells and in cultured S2 cells are reduced upon dopamine treatment, and increased in the presence of 3-IT. Moreover, the transducer of Btl signaling, MAP kinase, is hyper-activated throughout the tracheal tube in the *Pu* mutant. Finally we show that dopamine regulates endocytosis via controlling the dynamin protein level.

Keywords

Drosophila; trachea; dopamine; *Punch*; *pale*; *Catsup*; *breathless*; endocytosis; GTP cyclohydrolase; tyrosine hydroxylase

Introduction

The development of the *Drosophila* tracheal system, an extensively branched system of oxygen delivery tubes, models the patterning of vasculature in mammalian angiogenesis, both in cellular mechanisms of directed migratory behavior and in the conserved roles of numerous

*Corresponding authors. T.H. is to be contacted at fax: 01-843-792-5002; J.M.O. is to be contacted at fax: 01-205-348-1786. E-mail addresses: hsut@musc.edu (T.H.), jodonnel@bama.ua.edu (J.M.O.).
[1]These authors contributed equally to this work.
[2]Current address: Department of Pathology, Buffalo General Hospital, 100 High Street, Buffalo, NY14203, USA.

gene products (for reviews, see Metzger and Krasnow 1999; Affolter and Shilo 2000; Ghabrial et al. 2003). Detailed genetic analysis of *Drosophila* tracheal development has led to the identification of more than thirty genes (Affolter and Shilo 2000) engaged in patterning this complex structure. In both flies and mammals, the key defining process is the outgrowth of branches, regulated by growth factor signaling pathways. In *Drosophila*, the fibroblast growth factor (FGF) signaling pathway is utilized repeatedly to pattern the trachea in a stereotyped fashion with branching occurring in distinct stages: the primary and secondary branching forming through a tightly regulated genetic program (Metzger and Krasnow 1999) and tertiary branching arising in response to tissue oxygen demand (Wigglesworth 1959; Jarecki et al. 1999). The tracheal network arises during embryogenesis from laterally and segmentally repeated placodes each of 80-100 cells. Tracheal cells express the FGF receptor encoded by the *breathless* gene (*btl*; Lee et al. 1996). These cells migrate outward from a tracheal placodes in response to FGF (*Drosophila* Bnl, encoded by *branchless*) emanating from surrounding mesodermal cells (Sutherland et al. 1996). The entire tracheal architecture is formed by cell elongation, migration and rearrangement without further cellular division (Metzger and Krasnow 1999; Affolter and Shilo 2000), making it an ideal system for studying tubular cell migration. Disruption of FGF-FGFR signaling has a direct effect on tracheal tubule formation. Misexpression of *bnl* from sources other than the abutting mesodermal cells causes migration of tracheal cells to the ectopic source (Sutherland et al. 1996; Ribeiro et al. 2002), while expression of a constitutively active Btl receptor can cause the sprouting of supernumerary branches (Lee at al. 1996).

In the course of examining developmental roles of genes that regulate the biosynthesis of catecholamines, dopamine (DA) in particular, we found that abnormal embryonic tracheal patterning was a common mutant phenotype for these genes (Reynolds and O'Donnell 1987). This is surprising, since more typically, DA serves as a neurotransmitter and neurohormone in *Drosophila*, as in mammals, although previous studies in both *Drosophila* and mammals have implicated catecholamines in developmental processes such as embryonic nuclear division and ovarian development (Chen et al. 1994; Neckameyer 1996; Pendleton et al. 1996; Mayerhofer et al. 1997; Neckameyer et al. 2001; Pendleton et al. 2005) such as embryonic nuclear division and ovarian development.

The DA biosynthesis machinery is highly conserved in mammalian and *Drosophila* systems. DA production requires the tightly regulated collaboration of two enzymatic pathways. The DA pathway itself is initiated by the conversion of tyrosine to L-3-4-dihydroxyl-phenylalanine (L-Dopa), which is subsequently converted to DA (Nagatsu et al. 1964; Axelrod 1971). The rate-limiting step in the pathway, conversion of tyrosine to L-Dopa, is catalyzed by the enzyme tyrosine hydroxylase (TH), which is encoded by *pale* (*ple*) in *Drosophila* (Neckameyer and White 1993). Human and *Drosophila* TH share 60% amino acid similarity (Neckameyer et al. 2005). TH catalytic activity requires and is regulated by the cofactor, tetrahydrobiopterin (BH_4), synthesized via the pteridine pathway (Krishnakumar et al. 2000). The initiating and limiting component of BH_4 biosynthesis, and therefore, of DA production, is the activity of the enzyme GTP cyclohydrolase I (GTPCH). The human and *Drosophila* GTPCH proteins share 80% similarity (McLean et al. 1993). Mutations in the *Drosophila GTPCH* gene *Punch* (*Pu*) result in dose-dependent deficiencies in DA pools (Mackay et al. 1985; Weisberg and O'Donnell 1986; O'Donnell et al. 1989; Krishnakumar et al. 2000). Similarly, mutations in the human *GTPCH* locus lead to the hereditary diseases hyperphenylalaninemia and Dopa-responsive dystonia (reviewed in Thöny et al. 2000). Both *Pu* and *ple* mutations are homozygous lethal during embryogenesis. A third regulatory gene of DA synthesis, *Catecholamines up* (*Catsup*), acts as a negative regulator of both GTPCH and TH. The protein encoded by *Catsup* contains seven predicted transmembrane domains and functions in post-translational modification of both enzymes. Homozygous loss-of-function alleles of *Catsup*

also show developmental defects and die in an allele-dependent fashion, from embryogenesis to pupariation (Stathakis et al. 1999).

Here we demonstrate a role for the DA biosynthesis pathway genes in regulation of tubule migration in *Drosophila* trachea, and report new findings that the action of these genes is mediated via dopamine by controlling FGFR endocytosis.

Materials and methods

Drosophila strains and genetics

The *Pu* mutant alleles employed in this study were generated in EMS mutagenesis screens. The genotypes of the strains are: *dp cn* Pu^{AA17} *a px sp/SM1, dp cn* Pu^{Z22} *a px sp/SM1*, and *shv b cn* $Pu^{K5\text{-}2}$ *bw/SM1*. The genetic characteristics of these strains are reported in Mackay et al. (1985) and Reynolds and O'Donnell (1988); all are homozygous lethal and arrest during late embryogenesis. The homozygous lethal ple^2 is a loss-of-function allele recovered in an EMS screen (Neckameyer and White 1993). The homozygous lethal $Catsup^{26}$ allele is a 600 base pair deletion derived from the mobilization of a 5' P-element insertion in $Catsup^{KO5042}$ (Stathakis et al. 1999). *Pu* and *Catsup* mutants were maintained in a *CyO-GFP* background by crossing mutant flies into a *w; In(2LR)noc[4L]Sco[rv9R],* b^1*/CyO, P{ActGFP}JMR1* balancer chromosome. Mutant fly stocks of awd^{j2A4} and shi^2 were obtained from the Bloomington Stock Center and $btl^{H82\Delta3}$ was a gift from D. Montell (Johns Hopkins University, Baltimore, MA; Lee et al. 1996). awd^{j2A4} is a single P-element insertion, resulting in a completely null genotype (Krishnan et al. 2001; Dammai et al. 2003). The insertion site has been mapped to the 5′ untranslated region by the *Drosophila* genome project (Spradling et al. 1999). Both awd^{j2A4} and $btl^{H82\Delta3}$ are homozygous lethal and are maintained by pairing with the balancer *TM3, P {ry+ t7.2 =*$HZ^{2.7}$*}DB2 Sb*. The DB2 reporter gene shows β-galactosidase (β-Gal) expression in the maxillary segment. shi^2 is a temperature-sensitive allele of *shibire* that encodes *Drosophila* dynamin (van der Bliek and Meyerowitz 1991). Genetic recombination was used to incorporate *1-eve-1*, a transgenic line expressing the *lacZ* reporter gene in all tracheal cells at all stages from the *trachealess* gene promoter (Perrimon et al. 1991; a gift from A. Brand, University of Cambridge, Cambridge, UK). Transheterozygous embryos of shi^2 or ple^2 with *1-eve-1* were generated by standard genetic crosses.

The *y w; btl-Gal4; UAS-GFP, UAS-lacZ* fly was constructed as a trachea marker strain. The *y w; btl-Gal4; UAS-btl::GFP* transgenic line expresses a Btl::GFP fusion protein in *btl*-expressing tissues, including trachea. It was provided to the Hsu lab by T. Kornberg (University of California, San Francisco) and has been characterized previously (Sato and Kornberg 2002; Dammai et al. 2003). Note that a dash (-) is used to denote a promoter/enhancer fusion with a reporter gene while a double colon (::) is used to denote an open-reading-frame fusion. For example, *btl-Gal4* designates the yeast *Gal4* cDNA downstream of the *btl* promoter; while *UAS-btl::GFP* designates a *btl/GFP* fusion protein coding sequence regulated by the yeast *UAS* enhancer element. The binary *Gal4/UAS* transgenic expression system has been described (Brand and Perrimon 1993).

To generate *Pu* transgenic strains, the wild type *Pu* open reading frame were cloned into the P-element transformation vector (p*UAST*) downstream of the *UAS* enhancer element. The resulting transformation vector was then purified and injected into w^{1118} embryos by Genetic Services® (Cambridge, MA) and transgenic animals were isolated using established methodology (Spradling and Rubin 1982). Expression of the transgenes in trachea was achieved by mating homozygous strains with *btl-Gal4* strains.

Punch rescue constructs *w, UAS-Pu;* Pu^{Z22}*/ CyO, P{actGFP}JMR1; +/+* and *w;* Pu^{Z22}*/ CyO, P{ActGFP}JMR1; btl-Gal4* were generated separately and crossed. Progeny with the genotype

w, UASPu/+; Pu^{Z22}/Pu^{Z22}; btl-Gal4/+ were then selected as embryos without constitutive (*actin*) GFP expression and subjected to further analysis.

Antibodies

Rabbit anti-*Drosophila* GTPCH antibodies (Chen et al. 1994) were purified using Protein Aagarose beads (BioRad, Hercules, CA) and concentrated to 10 mg/ml. A 1:4000 dilution was used for immunohistochemistry (IHC). The rabbit anti-Ple antibody has been described (Neckameyer et al. 2000; Neckameyer et al. 2001) and was used at 1:2,000. Guinea pig anti-Catsup antibody has been described (Stathakis et al. 1999) and was used at 1:2,500 dilution after preadsorption with wild-type embryos. The mouse monoclonal anti-dopamine antibody (AbCam) was used at 1:5000. The mouse monoclonal anti-dp-MAPK (Sigma) was used at 1:500. The mouse monoclonal antibody 2A12 was obtained from the Developmental Studies Hybridoma Bank (DSHB, University of Iowa) and used at a 1:3 dilution. Mouse monoclonal anti-*Drosophila* dynamin (Shibire) antibody (BD Biosciences) was used at 1:250 for embryos and 1:300 for S2 cells in IHC and 1:2000 in Western blotting. Mouse monoclonal anti-β-Gal (Sigma) was used at 1:3000 for IHC. Rabbit anti-GFP (AbCam) was used at 1:200 for S2 cells in IHC and 1:2000 for Western blotting. Mouse monoclonal anti-*Drosophila* Crumbs antibody (from DSHB, University of Iowa) was used at 1:4 dilution for IHC.

Western blot of embryonic extracts

Wild type and mutant embryos were collected from grape juice agar plates after 17 hours of egg-laying at 25C° and dechorionated in 50% bleach for 3 minutes. After rinsing in H_2O, embryos were sonicated for 8 seconds on ice in extraction buffer (50 mM HEPES, pH7.6, 100 mM KCl, 1 mM EGTA, 1 mM $MgCl_2$, 1% Triton X-100, 10% glycerol) with protease inhibitor (from Roche) and supernatants were collected after centrifugation at 3,000 x g for 20 min at 4 °C. 50 μg of protein extracts were run on 7% SDS-polyacrylamide gel, electro-blotted, probed with anti-*Drosophila* dynamin (Shibire) antibody at 1:2000 (BD Biosciences), and reprobed with anti-β-actin antibody at 1:10,000 (mouse monoclonal from Sigma). The intensity of the bands was quantified and the relative intensities of the dynamin bands were normalized against the actin loading control using the Kodak Gel Doc II Software.

Immunohistochemistry

Whole-mount immunohistochemistry followed standard procedures (Hsu et al. 2001; Dammai et al. 2003). For fluorescence staining, Alexa Fluor 488- or 546-conjugated secondary antibodies were used (Invitrogen/Molecular Probes) at 1:200 dilution in 2-hr incubation at room temperature. For color staining, biotin-conjugated secondary antibodies (Vector) were used at 1:1000 dilution in 2-hr incubation at room temperature. Color development used the VectaStain reagents following the manufacturer's instruction (Vector).

Pharmacological treatment of embryos

Wild-type and mutant embryos were collected for twenty minutes on fresh grape agar plates, following a 90-min pre-lay. Embryos were washed in 1x PBS and exposed to heptane for twenty seconds after which they were immediately soaked in 1x PBS or 1x PBS containing DA (0.1 M; from Sigma) or 3-IT (2 mg/ml; from Sigma) for 5 min. The dosages were pre-determined empirically to be sub-lethal. The embryos were then transferred to fresh agar plates, placed in a humid chamber, and incubated at 25 °C for 17-24 hr.

Drosophila *Schneider 2 (S2) cell culture and treatments*

S2 cells (obtained from American Type Culture Collection) were maintained in Schneider's media supplemented with 10% heat-treated FBS (Cambrex). For immunohistochemistry, they were grown on coverslides coated with poly-L-lysine and were transfected using

Lipofectamine 2000 (from Invitrogen) with p*UC-HygMT-btl::GFP* (as described in Dammai et al. 2003). Btl::GFP fusion protein expression was induced with 10 μM $CuSO_4$ for 2 hr. The cells were then treated with buffer, DA (final concentration 0.1 mg/ml) or 3-IT (final concentration 1 mg/ml) for 12 hr, fixed and stained for GFP (rabbit polyclonal from AbCam, used at 1:200) and *Drosophila* Dynamin (Shibire) (mouse monoclonal from BD Biosciences, used at 1:300). There was limited or no cell death at these drug dosages. S2 cell extracts were prepared and Western-blotted as described previously (Hsu et al. 2001), and probed with anti-GFP (rabbit polyclonal from AbCam, used at 1:2000) and reprobed with anti-*Drosophila* dynamin (Shibire) antibody (mouse monoclonal from BD Biosciences, used at 1:2000) and with anti-β-actin antibodies (mouse monoclonal from Sigma, used at 1:10,000). The intensity of the bands was quantified using the Kodak Gel Doc II Software.

Results

Punch is expressed in the trachea during the migratory phase of development

Specific expression of Punch in the trachea has been noted (Samakovlis et al. 1996; Chen 1995). However, the correlation between DA synthesis and tracheal development has not been explored. As a first step toward elucidating the role of Punch in tracheal development, we analyzed more closely its temporal and spatial expression patterns. For comparison, the tracheal cells were marked by a transgenic line *1-eve-1* that expresses β-Galactosidase (β-Gal) in all tracheal cells at all stages, under control of the *trachealess* promoter (Perrimon et al. 1991). Tracheal development starts at the embryonic stage 10 with the formation of 10 placodes on each side of the embryos. These ectodermal placodes start invaginating inward at stage 11 (*1-eve-1* in Fig. 1A) and begin to extend branches at stage 12. These branches continue to extend and connect with the neighboring subunits during stage 13 through stage 15, until the stereotypic network of primary and secondary tubules are formed at stage 16. We found that strong Punch expression in the trachea encompasses only the mid-phase of tracheal development. Compared with the pan-tracheal reporter expression in *1-eve-1*, Punch expression is transient. It starts weakly at stage 11 and becomes most abundant from stage 12 to stage 14, coinciding with the active phase of tracheal branch migration (Fig. 1A). It fades after stage 15, when tubule extension is complete. To determine more precisely the subcellular localization of Punch, the trachea were double-stained for Punch and the transmembrane protein Crumbs (Crb). Enlarged views of portions of individual tracheal subunits are shown in Figure 1B. At stage 12, Punch in the developing trachea completely overlaps with Crb, indicating localization at or near the cell periphery. The peripheral localization of Punch is maintained through stage 14, in addition to some intracellular staining (red staining; arrowhead in the inset). At stage 15, when tracheal lumen begins to expand, weak peripheral localization of Punch is still detectable (solid arrow in the inset), while staining is also seen in the lumen (empty arrow in the inset). Intracellular and lumen Punch expression becomes barely detectable at stage 16 (data not shown). The significance of lumen staining at stage 15 is not clear at this time but may reflect the role of L-Dopa in cross-linking lumen cuticles (Wright 1987) and that the Punch-containing enzymatic complex may function extracellularly for this developmental role.

We also detected tracheal expression of the other two DA synthesis pathway components Ple and Catsup (Fig. 1C). It should be noted that the expression of these genes includes strong maternal contributions (Stathakis et al. 1999;Neckameyer et al. 1993;Neckameyer et al. 2000). Thus, although the two antibodies have proved specific (Stathakis et al. 1999;Neckameyer et al. 2000;Neckameyer et al. 2001), immunostaining of the embryos shows general staining in multiple tissues. Nonetheless, above-background staining in the trachea can be observed (Fig. 1C, insets) throughout tracheal development for both proteins.

DA synthesis pathway mutants exhibit tracheal development phenotypes

Specific expression of Punch in the tracheal cells during branch migration suggests a role in tracheal morphogenesis. In our initial examination of the tracheal network, monoclonal antibody 2A12 against a lumen antigen was used (Fig. 1D). Compared to wild-type (*y w*; Fig. 1Da), *Pu* mutants show misdirected tubules and ectopic branching, in addition to disruption of the dorsal trunk (Figs. 1Db-c). These phenotypes were generated by multiple alleles and in both heterozygotes and homozygotes. The examples shown are embryos developed through stage 14-15, as judged by well-developed midgut (not shown), in order to avoid secondary effects from early embryonic defects. These ectopic branching phenotypes are similar to those observed in mutants of *Drosophila* metastasis suppressor *Nm23* homolog (*awd*) and *dynamin* (*shi*), which cooperate in internalizing and down-regulating FGFR (Btl) (Dammai et al. 2003;Figs. 1Dd-e). By contrast, mutants of *Catsup*, which antagonizes *Pu*, exhibit phenotypes lacking tracheal branches. These lack-of-migration phenotypes of *Catsup* mutants range from a few gaps in the dorsal trunk (Fig. 1Df) to an almost complete lack of tubule formation (Fig. 1Dg). No *Pu*-like ectopic branches are observed in these mutants. The *Catsup* phenotypes are reminiscent of those observed in the *btl* mutants (see Fig. 1Dh as an example; Lee et al. 1996).

DA synthesis pathway gene functions regulate tracheal cell migration

Lumen staining using 2A12 monoclonal antibody is useful for observing overall structure of the tracheal network, but the cellular behavior underlying the branching defects cannot be discerned. For example, gaps in the dorsal trunk may result from mis-directed tubule migration that fails to connect with the lateral subunits (ectopic migration) or from lack of migration. That is, apparently similar phenotypes can result from opposite cellular behaviors. We therefore combined the mutant genes of interest with the *1-eve-1* transgene that marks all tracheal cells. *1-eve-1* alone showed limited or no tracheal phenotype (Dammai et al. 2003; Fig. 2A). In *Pu* mutants, ectopic looping and branch migration are observed (Fig. 2B-C). Importantly, in severely disrupted trachea, gaps in the dorsal trunk are always accompanied by mis-directed tracheal cells (arrow in Fig. 2C). These phenotypes are similar to those observed in the *shi* and *awd* mutants (Fig. S1) that are known to result in ectopic migration (Dammai et al. 2003). In the most extreme cases there was a complete loss of tracheal network while rounded “run-away” tracheal cells were seen throughout the embryos (Fig. 2D). Note that for these phenotypic analyses, we only documented late-stage embryos with developed body parts such as gut (empty arrowhead in Fig. 2C) or mandible structures (brackets in Fig. 2C and 2D), in order to avoid complications from early embryonic defects. The *Pu* phenotypes can be rescued by exogenously expressing a *UAS-Pu* transgene controlled by *btl-GAL4* in the trachea (Fig. 2E), even at the suboptimal expression temperature of 18°. Incubation at 25° resulted in a greater extent of rescue (fewer ectopic migration phenotypes) and the appearance of the opposite phenotype (lack of migration). Induction of opposite phenocopies by loss-of-function and over-expression of *Pu* strongly supports the notion that *Pu* has a specific dosage-dependent role in regulating tubule migration. These results indicate that the tracheal phenotypes in *Pu* mutants are the result of defective *Pu* function in the trachea, not indirect effects from early patterning or from neighboring tissues. The effectiveness of the transgene expression was confirmed by measuring the tyrosine hydroxylase activity in the embryonic extracts (Supplementary Fig. S2). Conversely, the *Catsup* mutant showed lack-of-migration phenotypes similar to that in *btl* mutants (Figs. 2F-G and Fig. S1). Note that there are no ectopic tracheal cells emanating from the tracheal tube ends at the gaps of dorsal trunk, indicating that these gaps result from lack of migration, not ectopic migration.

Interestingly, heterozygous mutants of *ple* showed similar ectopic migration phenotypes (Fig. 2H) as in *Pu* mutants. Note that heterozygous *ple* was examined for tracheal phenotypes because homozygous *ple* exhibited severe early embryonic defects. Besides ectopic migration

phenotypes, we often observed in *ple* mutants (Fig. 2I), and less frequently in *Pu* mutants (Fig. 2B), the appearance of convoluted dorsal trunks. Such phenotypes have been linked to defects in secretion and deposition of cuticle chitin in the tracheal lumen (Luschnig et al. 2006;Wang et al. 2006). It is therefore worth noting that L-Dopa, the direct enzymatic product of Pale/TH, is required for cuticle cross-linking (Wright 1987). However, cuticle deposition and lumen formation are initiated at late stage 14. As such, this aspect of the *Pu* and *ple* function is temporally distinct from the earlier tubule migration function.

DA directly regulates tracheal cell migration

Since the product of Punch/GTPCH enzymatic function, BH_4, is a cofactor of the Pale enzyme (TH), which in turn is a rate-limiting enzyme in the DA synthesis pathway, the similar tracheal phenotypes observed in *Pu* and *ple* mutants suggest that DA itself may play a role in modulating tracheal development. Indeed, DA is enriched in the wild-type trachea (Fig. 3A) but is absent in the *Pu* mutant (Fig. 3B). The pattern is consistent with the enrichment of Pu in tracheal cells (Fig. 1A). We next examined whether DA has a direct role in tubulogenesis. In this assay, a transgenic line expressing a GFP reporter gene driven by the *btl* enhancer was used to allow for examination of live embryos. The *Catsup* (lack of migration) and *Pu* and *ple* (ectopic migration) phenotypes were reproduced by DA and 3-iodotyrosine (3-IT, a TH inhibitor) treatments, respectively (Fig. 3C-F). Note that the dosages of DA and 3-IT were sublethal as the embryos developed normally into late stages. DA treatment resulted in gaps in the dorsal trunk (empty arrow in Fig. 3D) accompanied by clumps of tracheal cells that did not migrate out of the dorsal trunk (empty arrowheads in Fig. 3D). The clumping of tracheal cells in the dorsal trunk is in contrast to the normal and 3-IT treated samples that show clear and hollow lumenal space (sharp arrows in Figs. 3C and 3E). This phenotype is consistent with reduced tracheal cell migration. By contrast, in 3-IT treated embryos, misdirected branches (arrow in Fig. 3E) and ectopically localized tracheal cells were observed (bracket in Fig. 3E). The mislocalized tracheal cells are rounded and are not organized into tubule structures. All phenotypic classes generated by DA and 3-IT are summarized in Figure 3F. They are consistent with the lack-of-migration (DA treatment) and ectopic migration (3-IT treatment) mutant phenotypes described in Figure 2.

DA synthesis pathway regulates internalization of Btl receptor

We have previously shown that *awd* and *shi* cooperate in internalizing Btl, thus limiting the chemotactic signaling strength (Dammai et al. 2003). The striking phenotypic similarities between *Pu*/*ple* and *awd*/*shi*, as well as between *Catsup* and *btl*, suggest that DA synthesis pathway components may also modulate the FGFR signaling. If this hypothesis is correct, *Pu* and *ple* mutants are expected to increase the FGFR level, resulting in ectopic migration, while in *Catsup* mutants, the FGFR level should be down-regulated, resulting in reduced migration. Therefore, *Pu* should exacerbate, and *Catsup* rescue, the phenotypes of *awd* and *shi*; while reduced dosage of FGFR (in *btl* mutant) should rescue *Pu* but exacerbate *Catsup*. Since we have observed that the tracheal developmental functions of these genes of interest are partially haplo-insufficient (Dammai et al. 2003; data not shown), a simple transheterozygous analysis was conducted. All mutant alleles are marked with the *1-eve-1* transgene for visualizing tracheal cells. The severity and characteristics of ectopic migration and lack-of-migration phenotypes are defined in Figures 2 and Supplemental Figure S1. As shown in Table 1, Pu^{AA17} and awd^{j2A4} heterozygotes showed 84% and 81% mutant embryos with ectopic migration defects, respectively, while combined heterozygous and hemizygous shi^2 (progenies of X-linked homozygous shi^2 females crossed with wild-type males) showed 90% embryos with ectopic migration phenotypes. Transheterozygotes of Pu^{AA17}-awd^{j2A4} and Pu^{AA17}-shi^2 (the latter includes hemizygous shi^2) resulted in 100% penetrance with greatly enhanced severity. Conversely, $btl^{H82\Delta3}$ and $Catsup^{26}$ heterozygotes showed 84% and 67% embryos with lack-of-migration phenotypes, respectively, while $btl^{H82\Delta3}$-$Catsup^{26}$

transheterozygotes resulted in 100% penetrance for the same phenotype and with enhanced severity. When mutations generating opposite phenotypes were combined, as in Pu^{AA17}-$btl^{H82\Delta3}$ or $Catsup^{26}$-awd^{j2A4} transheterozygotes, the resulting severity of the respective phenotypes was greatly reduced. The same analyses were performed with another *Pu* allele Pu^{Z22} and they showed the same pattern of genetic interactions. As a validation of the genetic interaction scheme, we combined heterozygous *Catsup* with either of the two *Pu* alleles; the transheterozygotes showed improved ectopic or lack of migration phenotypes. In summary, *btl* allele can rescue different *Pu* alleles but *Pu* phenotypes are exacerbated by *awd* and *shi*. By contrast, the *Catsup* phenotype was exacerbated by *btl* but rescued by *awd*.

To examine whether dopamine synthesis mutants affect Btl/FGFR signaling, we examined the activity of MAP kinase (MAPK), the main transducer of FGFR signaling, within the tracheal cells. In wild-type (*1-eve-1*), activated MAPK (doubly-phosphorylated MAPK, dp-MAPK), is detected only in the migrating tip cells (arrowheads in Fig. 4A). In *Pu* mutants (Fig. 4B and 4C), there is significantly elevated levels of dp-MAPK in all tracheal cells, concomitant with ectopic migration phenotype. By contrast, in *Catsup* mutant, dp-MAPK is not detected in all tracheal cells, especially at the stunted tracheal tube ends (empty arrows in Fig. 4D). Therefore, the *Pu* ectopic migration phenotype can be correlated with the increased MAPK activity, while the *Catsup* lack-of-migration phenotype is consistent with reduced MAPK activity.

The observed genetic interactions between *Pu* and endocytic pathway mutants (*awd* and *shi*) raised the interesting prospect that DA synthesis pathway may also be involved in Btl/FGFR endocytosis in tracheal cells. To test this model, we first examined the expression of a Btl::GFP fusion protein expressed in the trachea. This fusion protein has been used in previous studies and has been shown to be functional (Sato and Kornberg 2002; Dammai et al. 2003). In the wild-type (*1-eve-1*) embryo without treatment, there is localization of Btl::GFP at the cell periphery as well as localization in intracellular vesicles (Fig. 5A). With DA treatment, there is a significant reduction in membrane Btl::GFP and a concomitant increase in the Btl::GFP-containing vesicles, both in size (arrowheads in Fig. 5B) and in number (Fig. 5D). By contrast, when the embryos are treated with 3-IT, there is an increased level and a more defined appearance of the peripheral Btl::GFP (i.e. sharper outlines of the tracheal cells; arrows in Fig. 5C) and a decrease in intracellular vesicular Btl::GFP (Fig. 5D).

To better quantify the response of Btl-GFP expression levels to drug treatments, we repeated the assays in cultured *Drosophila* cells (Fig. 6A). In untreated S2 cells stably transfected with the *btl::GFP* vector, the Btl::GFP fusion protein is present mostly in the cytoplasm with some surface localization. DA treatment resulted in reduction of Btl::GFP while 3-IT treatment resulted in increased accumulation of Btl::GFP in the cell periphery. Changes in total Btl::GFP levels upon drug treatments were confirmed by Western blotting (Fig. 6B, top panels). Taken together, it appears that DA can promote internalization and down-regulation of Btl while blocking DA synthesis results in over-accumulation of Btl.

DA regulates the level of dynamin

The results so far indicate that the function of *Pu* in tracheal morphogenesis is mediated through the action of DA, which in turn promotes internalization and turnover of the chemotactic receptor Btl/FGFR. To further explore the role of Pu and DA in regulating the endocytic pathway, we first examined the expression of Shi/dynamin in DA or 3-IT treated cells. As shown in Fig. 6A (middle panel), DA treatment resulted in increase of Shi/dynamin levels in S2 cells with pronounced peripheral localization (arrows), while 3-IT caused a dramatic reduction. The change of dynamin expression levels is confirmed by Western blotting (Fig. 6B, middle panels). We next examined whether this regulatory event occurs in the trachea (Fig. 7A). In wild-type (*1-eve-1*) embryos, Shi shows enriched expression in tracheal cells, and within the tracheal cells, Shi is abundant at the cell periphery. DA treatment results in a slight

enrichment of the peripheral localization in tracheal cells as well as in the neighboring non-tracheal cells. In *Pu* mutants, Shi expression is diffused and reduced. DA treatment rescued the Shi protein expression level in the *Pu* mutant. Importantly, we show that DA treatment could also rescue the tracheal defects in *Pu* mutants (Fig. 7B). To confirm that the Shi/dynamin expression is regulated by the DA synthesis pathway components *in vivo*, we examined the Shi/dynamin protein levels in the embryonic extracts from different mutants. As shown in Figure 7C, the two *Pu* mutants show 40-60% reduction in Shi/dynamin. The ple^{2} allele, a hypomorph, show 23% reduction while the $Catsup^{26}$ allele show an 83% increase.

Discussion

DA regulates cell migration

In this report, we demonstrate that genes involved in DA biosynthesis also regulate tracheal cell migration, and that this function is mediated by DA. This is unexpected since DA is normally associated with neuronal function. However, we believe this novel developmental function is not fortuitous because of the strong and highly specific expression of Punch in tracheal cells during the migratory phase of tracheal development (Fig. 1). In addition, the ectopic migration tracheal phenotypes in *Pu/GTPCH* mutants can be rescued by expressing a *Pu/GTPCH* transgene in developing trachea using a *btl* promoter, demonstrating the trachea-specific function of the DA pathway (Fig. 2E). Moreover, the expression of this transgene shows a dosage-dependent progression of phenotypic outcomes. That is, mild expression rescues ectopic migration, while over-expression tips the balance to blocked migration.

The product of GTPCH enzymatic activity, BH_4, is also a stabilizing cofactor of nitric oxide synthase (NOS), which is needed for hypoxia-induced outgrowth of terminal tracheal branches (Jarecki et al. 1999; Wingrove and O'Farrell 1999). However, the *Pu* mutant phenotypes reported here are most likely unrelated to this developmental process because of the following reasons: (1) Terminal branching occurs near the end of embryogenesis and during larval development (Jarecki et al. 1999; Wingrove and O'Farrell 1999) whereas the defects in primary and secondary branch migration occur during midembryogenesis. (2) Mutations in *ple*, which has no role in NOS function, also results in ectopic migration phenotypes (Fig. 2H). (3) DA and the DA pathway inhibitor can phenocopy the genetic mutants (Fig. 3). (4) DA treatment can rescue *Pu/GTPCH* mutant phenotypes (Fig. 7B), implicating a direct role of DA in primary and secondary branch migration. Interestingly, DA is enriched in the trachea (Fig. 3).

An inhibitory role for DA in the regulation of cell migration has been reported for a number of cell types over recent years. Yasunari et al. (1997; 2003) have demonstrated that DA is capable of blocking the migration of vascular smooth muscle cells, a factor in the formation of atherosclerotic lesions, in a process mediated through the D1 class of DA receptors. DA also was reported to interfere with activated neutrophil transendothelial migration (Sookhai et al. 2000). Similarly, DA, acting through D1 receptors, is reported to reduce the migration of regulatory T cells in damaged neural regions, thereby providing protection against T cell-mediated neurodegeneration (Kipnis et al. 2004). Finally, DA acting through the D2 class of DA receptors, can inhibit tumor angiogenesis in highly vascularized gastric and ovarian tumors (Basu et al. 2001, 2004; Chakroborty et al. 2004). It would be interesting to determine whether the mammalian GTPCH-TH-DA enzymatic pathways also have a non-neurological function in modulating tubulogenesis during development.

The modulation of surface FGFR by DA is dynamin-dependent

We found that DA pathway mutants show tracheal abnormalities that are strikingly similar to the perturbations of tracheal cell migration in embryos with abnormalities in FGF signaling. Diminution of DA expression in *Drosophila* embryos, either by mutations (*Pu* and *ple*) or by

pharmacological depletion (3-IT treatment), has dramatic effects on the stereotyped migratory behavior of tracheal cells and patterning of the resulting branched structure. We observed that entire branches are misdirected and individual cells move away from the tracheal branches, a phenotype we term “run-away cells”. Under conditions of excess DA, via mutations (*Catsup*) or pharmacological modification (DA treatment), the converse phenotype, one of blocked migration, is evident. This phenotype is often associated with clustering of tracheal cells near the stunted ends of tracheal tubes. These opposing phenotypes are correlated with the increased or decreased levels of MAPK activation, the mediator of FGFR signaling (Fig. 4).

Our data further demonstrate that DA regulates FGF receptor turnover. We show that Btl::GFP fusion protein is down-regulated in the presence of DA and up-regulated in the presence of 3-IT, either in trachea or in cultured S2 cells (Figs. 5 and 6). These results are consistent with the model that DA promotes internalization of Btl/FGFR, leading to its degradation through the endocytic pathway. The role of DA in internalization of FGFR is further suggested by the genetic interaction between the DA synthesis and endocytic pathway genes. Mutations in the human tumor suppressor nucleoside diphosphate kinase (NDK) gene (*nm23*) are strongly associated with tumor metastatic activity (Steeg et al. 1988;Freije et al. 1997). Its functional homolog in *Drosophila*, *abnormal wing discs* (*awd*) (Biggs et al. 1990), has been shown to genetically interact with a temperature-sensitive allele of the *shibire* gene (shi^{ts}), which encodes dynamin (Krishnan et al. 2001), a large GTPase required for the formation of clathrin-coated endocytic vesicles (Kosaka and Ikeda 1983;van der Bliek and Meyerowitz, 1991). Dammai et al. (2003) first demonstrated a function for *awd/nm23* in the migratory phase of tracheal development and functional interactions with *shi/dynamin* that are required for the modulation of FGFR/Btl levels in tracheal cells. In this report, we show that *Pu* and *ple* phenotypes are exacerbated by *awd* and rescued by *btl*, while the *Catsup* phenotypes are rescued by *awd* but exacerbated by *btl* (Table 1). These results indicate that Pu/GTPCH and Ple/TH, and by extension, DA, are positive regulators of endocytosis.

We have extended this analysis by implicating direct involvement of DA in regulating the Shi/dynamin protein itself. Mutations in *Pu/GTPCH*, which regulates DA pools (Krishnakumar et al. 2000), result in reduction of the Shi/dynamin levels (Fig. 7) and, in consequence, the subsequent accumulation of FGFR/Btl in the plasma membranes of tracheal cells, thus accounting for ectopic migratory behavior of these mutant cells. Importantly, down-regulation of Shi/dynamin level in the *Pu* mutants can be rescued by treatment with DA. A direct correlation between DA and dynamin levels is also demonstrated in cultured S2 cells (Fig. 6). Thus, the genetic and pharmacological evidence in this report supports the hypothesis that the diminished DA pools that accompany loss-of-function mutations in the *Pu/GTPCH* and *ple/TH* genes result in deficits of DA-mediated signaling necessary for Shi/dynamin accumulation. The function of the DA synthesis pathway component in tracheal cell migration is illustrated in Figure 8.

Evidence of a role of DA in receptor endocytosis has emerged recently. For instance, DA can promote VEGFR endocytosis in cultured human endothelial cells (Basu et al. 2001). DA D_3 receptor-mediated modulation of $GABA_A$ receptor (Chen et al. 2006) and DA-regulated endocytosis of the renal cell Na^+, K^+-ATPase (Efendiev et al. 2002) are similarly dynamin-mediated events. Why is a neurohormone also a mediator of endocytosis in other cell types? It is interesting to consider the possibility that the endocytic activity of DA may in fact be its ancestral function, which was adopted by the neurons and tubular cells later. Indeed, primitive, nerve-less multicellular organisms such as sponge can produce dopamine (Liu et al. 2004). The precise mechanism(s) by which DA regulates dynamin assembly is not yet clear. However, Efendiev et al (2002) reported that DA signaling promotes dynamin stabilization and assembly at the plasma membrane in cultured human kidney cells – and thus endocytosis – by activating

protein phosphatase 2A which dephosphoylates dynamin-2. It is possible that a similar mechanism of action occurs in the tracheal cells and future experiments will help to address this possibility.

Supplementary Material

Refer to Web version on PubMed Central for supplementary material.

Acknowledgments

We thank A. Brand, T. Kornberg, D. Montell, and the Drosophila Stock Center for providing fly strains. This work was supported by Abney Scholarship to A.H., National Cancer Institute grant to J.O. and T.H. (R21CA099021) and National Cancer Institute grant to T.H. (RO1CA109860).

References

Affolter M, Shilo BZ. Genetic control of branching morphogenesis during Drosophila tracheal development. Curr Opin Cell Biol 2000;12:731–5. [PubMed: 11063940]

Axelrod J. Noradrenaline: fate and control of its biosynthesis. Science 1971;173:598–606. [PubMed: 4397955]

Basu S, Nagy JA, Pal S, Vasile E, Eckelhoefer IA, Bliss VS, Manseau EJ, Dasgupta PS, Dvorak HF, Mukhopadhyay D. The neurotransmitter dopamine inhibits angiogenesis induced by vascular permeability factor/vascular endothelial growth factor. Nat Med 2001;7:569–74. [PubMed: 11329058]

Basu S, Sarkar C, Chakroborty D, Nagy J, Mitra RB, Dasgupta PS, Mukhopadhyay D. Ablation of peripheral dopaminergic nerves stimulates malignant tumor growth by inducing vascular permeability factor/vascular endothelial growth factor-mediated angiogenesis. Cancer Res 2004;64:5551–5. [PubMed: 15313889]

Biggs J, Hersperger E, Steeg PS, Liotta LA, Shearn A. A Drosophila gene that is homologous to a mammalian gene associated with tumor metastasis codes for a nucleoside diphosphate kinase. Cell 1990;63:933–40. [PubMed: 2175255]

Brand AH, Perrimon N. Targeted gene expression as a means of altering cell fates and generating dominant phenotypes. Development 1993;118:401–15. [PubMed: 8223268]

Chakroborty D, Sarkar C, Mitra RB, Banerjee S, Dasgupta PS, Basu S. Depleted dopamine in gastric cancer tissues: dopamine treatment retards growth of gastric cancer by inhibiting angiogenesis. Clin Cancer Res 2004;10:4349–56. [PubMed: 15240521]

Chen G, Kittler JT, Moss SJ, Yan Z. Dopamine D3 receptors regulate GABAA receptor function through a phospho-dependent endocytosis mechanism in nucleus accumbens. J Neurosci 2006;26:2513–21. [PubMed: 16510729]

Chen, X. Developmental expression and function analysis of GTP cyclohydrolase isoforms in *Drosophila melanogaster*. University of Alabama; 1995. Ph.D. dissertation

Chen X, Reynolds ER, Ranganayakulu G, O'Donnell JM. A maternal product of the *Punch* locus of *Drosophila melanogaster* is required for precellular blastoderm nuclear divisions. J Cell Sci 1994;107 (Pt 12):3501–13. [PubMed: 7706401]

Dammai V, Adryan B, Lavenburg KR, Hsu T. Drosophila awd, the homolog of human nm23, regulates FGF receptor levels and functions synergistically with shi/dynamin during tracheal development. Genes Dev 2003;17:2812–24. [PubMed: 14630942]

Efendiev R, Yudowski GA, Zwiller J, Leibiger B, Katz AI, Berggren PO, Pedemonte CH, Leibiger IB, Bertorello AM. Relevance of dopamine signals anchoring dynamin-2 to the plasma membrane during Na+,K+-ATPase endocytosis. J Biol Chem 2002;277:44108–14. [PubMed: 12205083]

Freije JM, Blay P, MacDonald NJ, Manrow RE, Steeg PS. Site-directed mutation of Nm23-H1. Mutations lacking motility suppressive capacity upon transfection are deficient in histidine-dependent protein phosphotransferase pathways in vitro. J Biol Chem 1997;272:5525–32. [PubMed: 9038158]

Ghabrial A, Luschnig S, Metzstein MM, Krasnow MA. Branching morphogenesis of the Drosophila tracheal system. Annu Rev Cell Dev Biol 2003;19:623–47. [PubMed: 14570584]

Hsu T, McRackan D, Vincent TS, Gert de Couet H. Drosophila Pin1 prolyl isomerase Dodo is a MAP kinase signal responder during oogenesis. Nat Cell Biol 2001;3:538–43. [PubMed: 11389437]

Jarecki J, Johnson E, Krasnow MA. Oxygen regulation of airway branching in Drosophila is mediated by branchless FGF. Cell 1999;99:211–20. [PubMed: 10535739]

Kipnis J, Cardon M, Avidan H, Lewitus GM, Mordechay S, Rolls A, Shani Y, Schwartz M. Dopamine, through the extracellular signal-regulated kinase pathway, downregulates CD4+CD25+ regulatory T-cell activity: implications for neurodegeneration. J Neurosci 2004;24:6133–43. [PubMed: 15240805]

Kosaka T, Ikeda K. Possible temperature-dependent blockage of synaptic vesicle recycling induced by a single gene mutation in Drosophila. J Neurobiol 1983;14:207–25. [PubMed: 6304244]

Krishnakumar S, Burton D, Rasco J, Chen X, O'Donnell J. Functional interactions between GTP cyclohydrolase I and tyrosine hydroxylase in *Drosophila*. J Neurogenet 2000;14:1–23. [PubMed: 10938545]

Krishnan KS, Rikhy R, Rao S, Shivalkar M, Mosko M, Narayanan R, Etter P, Estes PS, Ramaswami M. Nucleoside diphosphate kinase, a source of GTP, is required for dynamin-dependent synaptic vesicle recycling. Neuron 2001;30:197–210. [PubMed: 11343655]

Lee T, Hacohen N, Krasnow M, Montell DJ. Regulated Breathless receptor tyrosine kinase activity required to pattern cell migration and branching in the Drosophila tracheal system. Genes Dev 1996;10:2912–21. [PubMed: 8918892]

Liu H, Mishima Y, Fujiwara T, Nagai H, Kitazawa A, Mine Y, Kobayashi H, Yao X, Yamada J, Oda T, Namikoshi M. Isolation of Araguspongine M, a New Stereoisomer of an Araguspongine/Xestospongin alkaloid, and Dopamine from the Marine Sponge Neopetrosia exigua Collected in Palau. Mar. Drugs 2004;2:154–63.

Luschnig S, Batz T, Armbruster K, Krasnow MA. serpentine and vermiform encode matrix proteins with chitin binding and deacetylation domains that limit tracheal tube length in Drosophila. Curr Biol 2006;16:186–94. [PubMed: 16431371]

Mackay WJ, Reynolds ER, O'Donnell JM. Tissue-specific and complex complementation patterns in the *Punch* locus of *Drosophila melanogaster*. Genetics 1985;111:885–904. [PubMed: 3934035]

Mayerhofer A, Dissen GA, Costa ME, Ojeda SR. A role for neurotransmitters in early follicular development: induction of functional follicle-stimulating hormone receptors in newly formed follicles of the rat ovary. Endocrinology 1997;138:3320–9. [PubMed: 9231784]

McLean JR, Krishnakumar S, O'Donnell JM. Multiple mRNAs from the *Punch* locus of *Drosophila melanogaster* encode isoforms of GTP cyclohydrolase I with distinct N-terminal domains. J Biol Chem 1993;268:27191–7. [PubMed: 8262960]

Metzger RJ, Krasnow MA. Genetic control of branching morphogenesis. Science 1999;284:1635–9. [PubMed: 10383344]

Nagatsu T, Levitt M, Udenfriend S. Tyrosine hydroxylase. The initial step in norepinephrine biosynthesis. J Biol Chem 1964;239:2910–7. [PubMed: 14216443]

Neckameyer WS. Multiple roles for dopamine in Drosophila development. Dev Biol 1996;176:209–19. [PubMed: 8660862]

Neckameyer WS, Woodrome S, Holt B, Mayer A. Dopamine and senescence in *Drosophila melanogaster*. Neurobiol Aging 2000;21:145–52. [PubMed: 10794859]

Neckameyer W, O'Donnell J, Huang Z, Stark W. Dopamine and sensory tissue development in *Drosophila*. J Neurobiol 2001;15:280–94. [PubMed: 11351339]

Neckameyer WS, Holt B, Paradowski TJ. Biochemical conservation of recombinant Drosophila tyrosine hydroxylase with its mammalian cognates. Biochem Genet 2005;43:425–43. [PubMed: 16187166]

Neckameyer WS, White K. Drosophila tyrosine hydroxylase is encoded by the *pale* locus. J Neurogenet 1993;8:189–99. [PubMed: 8100577]

O'Donnell JM, McLean JR, Reynolds ER. Molecular and developmental genetics of the *Punch* locus, a pterin biosynthesis gene in *Drosophila melanogaster*. Dev Genet 1989;10:273–86. [PubMed: 2500290]

Pendleton RG, Rasheed A, Paluru P, Joyner J, Jerome N, Meyers RD, Hillman R. A developmental role for catecholamines in *Drosophila* behavior. Pharmacol Biochem Behav 2005;81:849–53. [PubMed: 16051344]

Pendleton RG, Robinson N, Roychowdhury R, Rasheed A, Hillman R. Reproduction and development in Drosophila are dependent upon catecholamines. Life Sci 1996;59:2083–91. [PubMed: 8950311]

Perrimon N, Noll E, McCall K, Brand A. Generating lineage-specific markers to study Drosophila development. Dev Genet 1991;12:238–52. [PubMed: 1651183]

Reynolds ER, O'Donnell JM. An analysis of the embryonic defects in *Punch* mutants of *Drosophila melanogaster*. Dev Biol 1987;123:430–41. [PubMed: 3115849]

Reynolds ER, O'Donnell JM. Characterization of new *Punch* mutations: identification of two additional mutant classes. Genetics 1988;119:609–17. [PubMed: 3136053]

Ribeiro C, Ebner A, Affolter M. In vivo imaging reveals different cellular functions for FGF and Dpp signaling in tracheal branching morphogenesis. Dev Cell 2002;2:677–83. [PubMed: 12015974]

Samakovlis C, Hacohen N, Manning G, Sutherland DC, Guillemin K, Krasnow MA. Development of the Drosophila tracheal system occurs by a series of morphologically distinct but genetically coupled branching events. Development 1996;122:1395–407. [PubMed: 8625828]

Sato M, Kornberg TB. FGF is an essential mitogen and chemoattractant for the air sacs of the Drosophila tracheal system. Dev Cell 2002;3:195–207. [PubMed: 12194851]

Sookhai S, Wang JH, Winter D, Power C, Kirwan W, Redmond HP. Dopamine attenuates the chemoattractant effect of interleukin-8: a novel role in the systemic inflammatory response syndrome. Shock 2000;14:295–9. [PubMed: 11028546]

Spradling AC, Rubin GM. Transposition of cloned P elements into Drosophila germ line chromosomes. Science 1982;218:341–7. [PubMed: 6289435]

Spradling AC, Stern D, Beaton A, Rhem EJ, Laverty T, Mozden N, Misra S, Rubin GM. The Berkeley Drosophila Genome Project gene disruption project: Single P-element insertions mutating 25% of vital Drosophila genes. Genetics 1999;153:135–77. [PubMed: 10471706]

Stathakis DG, Burton DY, McIvor WE, Krishnakumar S, Wright TR, O'Donnell JM. The Catecholamines up (Catsup) protein of *Drosophila melanogaster* functions as a negative regulator of tyrosine hydroxylase activity. Genetics 1999;153:361–82. [PubMed: 10471719]

Steeg PS, Bevilacqua G, Kopper L, Thorgeirsson UP, Talmadge JE, Liotta LA, Sobel ME. Evidence for a novel gene associated with low tumor metastatic potential. J Natl Cancer Inst 1988;80:200–4. [PubMed: 3346912]

Sutherland D, Samakovlis C, Krasnow MA. *branchless* encodes a Drosophila FGF homolog that controls tracheal cell migration and the pattern of branching. Cell 1996;87:1091–101. [PubMed: 8978613]

Thony B, Auerbach G, Blau N. Tetrahydrobiopterin biosynthesis, regeneration and functions. Biochem J 2000;347(Pt 1):1–16. [PubMed: 10727395]

van der Bliek AM, Meyerowitz EM. Dynamin-like protein encoded by the *Drosophila shibire* gene associated with vesicular traffic. Nature 1991;351:411–4. [PubMed: 1674590]

Wang S, Jayaram SA, Hemphala J, Senti KA, Tsarouhas V, Jin H, Samakovlis C. Septate-junction-dependent luminal deposition of chitin deacetylases restricts tube elongation in the Drosophila trachea. Curr Biol 2006;16:180–5. [PubMed: 16431370]

Weisberg EP, O'Donnell JM. Purification and characterization of GTP cyclohydrolase I from *Drosophila melanogaster*. J Biol Chem 1986;261:1453–8. [PubMed: 3080426]

Wigglesworth VB. The role of the epidermal cells in the 'migration' of tracheoles in *Rhodinus prolixus* (Hemiptera). J Exp Biol 1959;36:632–640.

Wingrove JA, O'Farrell PH. Nitric oxide contributes to behavioral, cellular, and developmental responses to low oxygen in *Drosophila*. Cell 1999;98:105–14. [PubMed: 10412985]

Wright TR. The genetics of biogenic amine metabolism, sclerotization, and melanization in *Drosophila melanogaster*. Adv Genet 1987;24:127–222. [PubMed: 3124532]

Yasunari K, Kohno M, Hasuma T, Horio T, Kano H, Yokokawa K, Minami M, Yoshikawa J. Dopamine as a novel antimigration and antiproliferative factor of vascular smooth muscle cells through dopamine D1-like receptors. Arterioscler Thromb Vasc Biol 1997;17:3164–73. [PubMed: 9409307]

Yasunari K, Maeda K, Nakamura M, Yoshikawa J. Dopamine as a novel anti-migration factor of vascular smooth muscle cells through D1A and D1B receptors. J Cardiovasc Pharmacol 2003;41(Suppl 1):S33–8. [PubMed: 12688394]

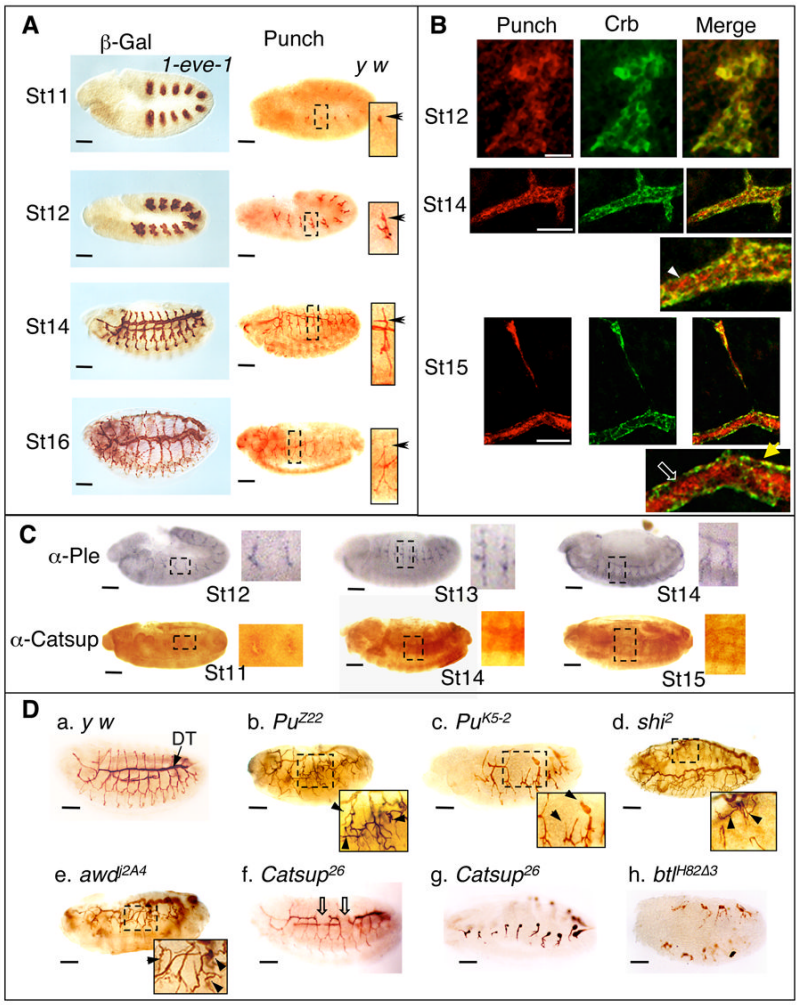

Fig. 1.

Pu and *Catsup* are involved in tracheal development. (A) Comparison of β-Gal (directed by the trachea-specific *trachealess* promoter) and Punch expression patterns in the trachea. β-Gal expression in *1-eve-1* marks all tracheal cells at all stages while Punch is expressed most abundantly in the trachea from stage 12 to stage 14. The insets show enlarged views of individual tracheal subunits stained for Punch. Arrows point to the site from which the dorsal trunk extends. The expression of Punch fades after stage 14. Bars are 50 μm. (B) Close-up views of portions of single tracheal subunits at stage 12, 14 and 15, double stained for Punch (red) and Crb (green). Crb is a transmembrane protein and Punch overlaps with Crb completely in the trachea at stage 12. At stage 14 Punch still shows extensive overlap with Crb in addition to some intracellular localization (arrowhead). At stage 15, peripheral localization of Punch is diminished (arrow) with an increased expression in the lumen (open arrow). Bars are 10 μm. (C) *y w* embryos were stained with anti-Ple or anti-Catsup antibodies, as indicated. The insets show enlarged views of two tracheal subunits with Ple or Catsup expression. The higher level of general staining indicate that the two proteins are expressed in multiple tissues. Bars are 10 μm. (D) Embryos of indicated genotypes were stained with a tracheal lumen-specific antibody 2A12. Unless specified, all embryos are oriented with anterior to the left and dorsal side up. (a) *y w* represents wild-type. The major tracheal branch that runs along the length of the embryo, dorsal trunk, is marked (DT). (b-c) Embryos homozygous for two *Pu* alleles *Z22* and *K5-2* show disrupted tracheal network. The insets highlight ectopic branches (arrowheads). (d)

shi^{2} temperature-sensitive mutant embryos were collected at 25° for 7 hr and then incubated at 30° for 7 hr. The inset highlights ectopic branches (arrowheads). (e) An *awd*^{j2A4} mutant. The inset highlights ectopic branches (arrowheads). (f-g) Two *Catsup*^{26} mutant embryos showing moderate and severe phenotypes, respectively. Empty arrows in (f) mark the gaps in the dorsal trunk, while (g) shows almost no branch migration. (h) Ventral view of a *btl*$^{H82\Delta 3}$ mutant embryo showing little branch migration. Bars are 50 μm.

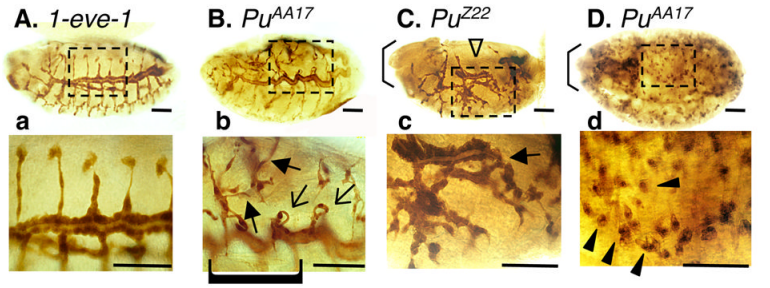

E.

Phenotypes	*Pu*^{Z22}; *btl-GAL4* at 25° (%) (n=27)	*UAS-Pu/+; Pu*^{Z22}; *btl-GAL4/+* at 18°C (%) (n=42)	*UAS-Pu/+; Pu*^{Z22}; *btl-GAL4/+* at 25°C (%) (n=38)
Ectopic migration	81.4	21.4	15.8
Normal	18.5	78.5	68.3
Lack of migration	—	—	15.8

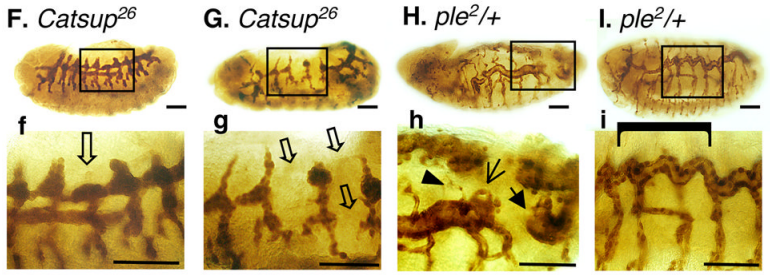

Fig. 2.

Tracheal cell migration defects in DA synthesis pathway mutants. The embryos were stained for β-Gal. Unless specified, all mutants are homozygotes marked by the *1-eve-1* transgene that expresses β-Gal under control of the *trachealess* promoter. All embryos are oriented with anterior to the left and dorsal side up. (A) *1-eve-1* represents wild-type. (B-D) Mutant embryos homozygous for two *Pu* alleles *AA17* and *Z22*. In inset (Bb), arrows point to ectopically migrating branches and tracheal cells. Sharp arrows point to ectopic looping of the dorsal branches. Bracket marks convoluted dorsal trunk. (Cc) shows severe disruption of the tracheal network with abnormal branching and sprouting. Arrow points to the misguided branch emanating from the truncated dorsal trunk. (Dd) shows a severe *Pu* mutant; rounded "run-away" tracheal cells can be identified (arrowheads). (E) Rescue of *Pu* phenotypes by *Pu* transgene expression in trachea. Wild-type *Pu* expression in *Pu* mutant background gives three broad phenotypic classes as indicated. *w; Pu*^{Z22}*/Pu*^{Z22}*; btl-Gal4 or w, UAS-Pu; Pu*^{Z22}*/Pu*^{Z22}*; +/+* each gave similar distribution of phenotypes, thus only *w; Pu*^{Z22}*/Pu*^{Z22}*; btl-Gal4* was tabulated as the parental *Pu* mutant. The above two lines were crossed to generate the rescue lines, as described in Materials and Methods. The embryos were incubated at 18° or 25° to control the expression level of the *Pu* transgene. (F-G) Mild and severe phenotypes of *Catsup* mutant showing missing branches and stunted branch migration. Note that there is no ectopic branching at or near the gaps in tracheal tubes in these mutant, indicating loss-of-migration. (H) A *ple* heterozygote showing moderate tracheal phenotypes similar to those in *Pu* mutants. (Hh) Sharp arrow points to ectopic looping, arrow points to ectopically migrating branches at the breakage point and arrowhead points to ectopically migrating cells. (I) A *ple* heterozygote showing convoluted tracheal trunk (bracket). Bars are 50 μm.

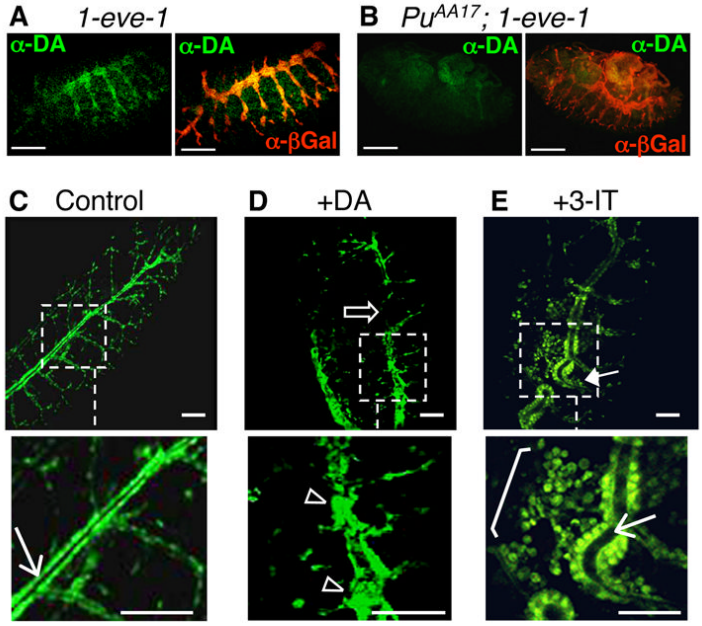

F

Dopamine-treated embryos (n=43)	
Phenotypic class	**Distribution**
1. Normal	46.5%
2. Mild dorsal trunk breakage	16.3%
3. Multiple dorsal trunk breaks, with cell clumping	27.9%
4.Severely deformed, early arrest in cell migration	9.3%
3-IT-treated embryos (n=40)	
Phenotypic class	**Distribution**
1. Normal	45.0%
2. Rounded tracheal cells near primary branches	5.0%
3. Ectopic branching	12.5%
4. Dorsal trunk disruptions, accompanied by aberrant cell migration	37.5%

Fig. 3.

Tracheal development can be modified with DA and a TH inhibitor in wild-type embryos. (A-B) *1-eve-1* or Pu^{AA17}*; 1-eve-1* embryos were processed for double-staining with anti-DA (green) and anti-β-Gal (red) antibodies. DA is enriched in the wild-type trachea but absent in *Pu* mutant. (C-F) *y w* embryos carrying *btl-GAL4* and *UAS-GFP* transgenes were collected at 25 °C and mock treated (control) or treated with DA or 3-IT. Stage 15-16 embryos were examined under a fluorescence microscope. The GFP reporter gene is expressed in all tracheal cells. All embryos are shown with dorsal side on the left and anterior to the top. (C) A mock-treated embryo displays an orderly patterning of tracheal architecture. The sharp arrow points to well-formed lumen. (D) A DA-treated embryo showing a gap in the dorsal trunk (empty

arrow). The enlarged view shows accumulation of non-migrating cells (empty arrowheads) clustered in the dorsal trunk, obstructing the lumen. (E) A 3-IT treated embryo showing ectopic branches (arrow). The enlarged view shows ectopically located and abnormally shaped (rounded) tracheal cells (bracket). The sharp arrow points to a well-formed lumen. (F) Quantification of the above recorded phenotypes (C-E). The drug exposure protocol was optimized to ensure minimal early developmental defects and increased embryo viability. Only embryos surviving past stage 14 were counted. Scale bars in (A-B) are 10 μm; in (C-E) are 50 μm.

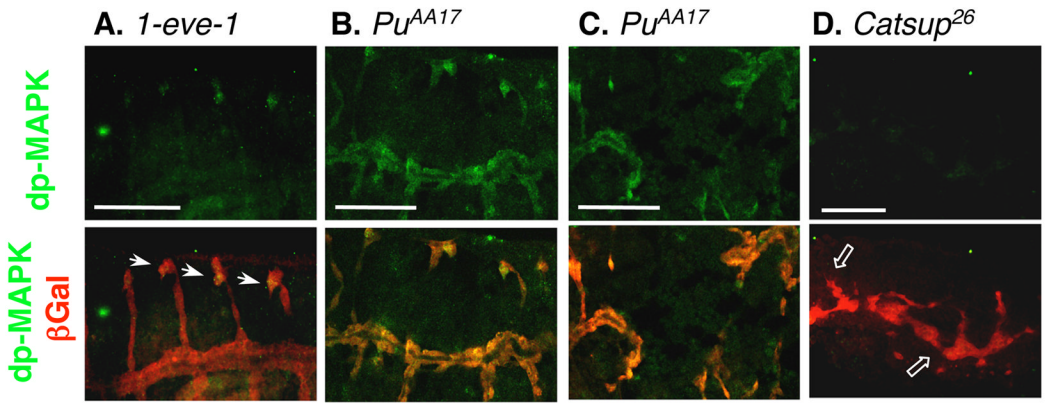

Fig. 4.

MAPK activation levels in DA synthesis pathway mutants. *1-eve-1*, Pu^{AA17}*; 1-eve-1*, or $Catsup^{26}$*; 1-eve-1* embryos were processed for double staining with anti-dp-MAPK and anti-β-Gal antibodies. In wild-type embryos (A), dp-MAPK is detected in the migrating tip cells (arrowheads). In *Pu* mutants (BC), dp-MAPK is over-expressed in all tracheal cells. In *Catsup* mutant embryos (D) dp-MAPK is not detectable in the tracheal cells, especially not in the stunted tube ends (empty arrows).

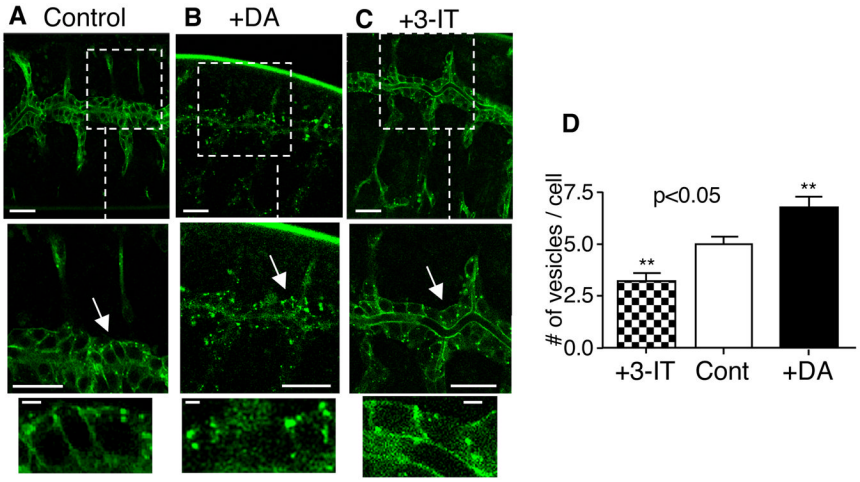

Fig. 5.

Dopamine promotes internalization of Btl receptor. (A-C) Embryos of transgenic flies *btl-GAL4; UAS-btl::GFP* were treated with buffer (control), DA or 3-IT and observed for Btl::GFP fusion protein expression. Anterior is to the left and the dorsal side is up. All images were acquired using identical settings to ensure accurate quantification. Middle panels show enlarged views of the indicated areas in top panels. Arrows in the middle panels point to the position of three cells further enlarged in the bottom panels. (A) A stage 15 embryo shows normal Btl-GFP distribution at plasma membrane and some cytoplasmic localization in vesicles. (B) A stage 15 embryo treated with DA. The level of membrane Btl-GFP is greatly reduced. (C) A stage 15 embryo treated with 3-IT. Btl::GFP shows more pronounced surface localization. (D) Quantification of vesicle numbers per cell in DA and 3-IT treated vs. control embryos. To avoid cell- and position-specific variations, GFP-containing vesicles are counted in cells at the same position of multiple embryos. Error bars show standard error (control, n=7 individual cells; 3-IT-treated, n=9 individual cells; DA-treated, n=8 individual cells; each data set was acquired from a minimum of 4 representative embryos). The 3-IT and DA treated embryos display significantly reduced and increased number, respectively, when compared to untreated control. ** denotes statistically significant differences as compared to the control ($p < 0.05$).

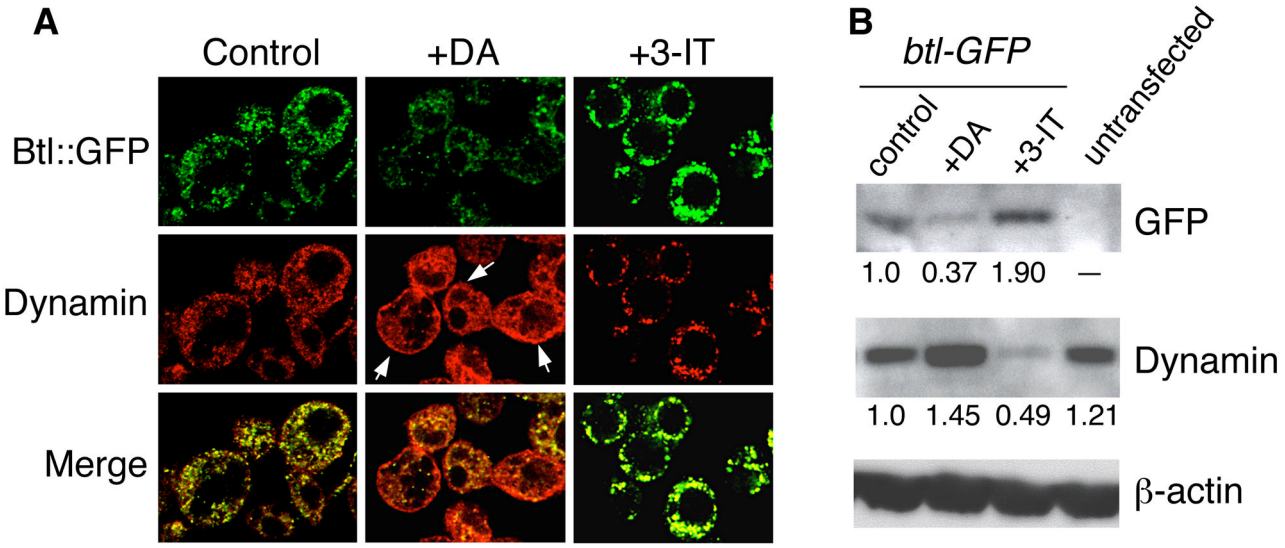

Fig. 6.

DA promotes endocytosis of Btl/FGFR in S2 cells. S2 cells were transfected with plasmids expressing Btl::GFP fusion protein, treated with the indicated agents and either (A) double stained for GFP and Shi/dynamin or (B) processed for Western blotting. (A) Without drug treatment (control), Btl::GFP fusion protein is mostly internal with some surface localization. These cells also express endogenous Shi/dynamin. DA treatment resulted in significant reduction in Btl::GFP level and an increase in Shi/dynamin level as well as more pronounced peripheral localization of Shi/dynamin (arrows). 3-IT treatment resulted in increased Btl::GFP level near the cell periphery and concurrent reduction in Shi/dynamin level. (B) Western blot for Btl::GFP (using anti-GFP antibody) and Shi/dynamin in lysates from the cells treated as in (A). The blot was reprobed for β-actin as a loading control. The numbers under the Btl:GFP and dynamin protein lanes indicate the relative protein levels (normalized to the β-actin controls).

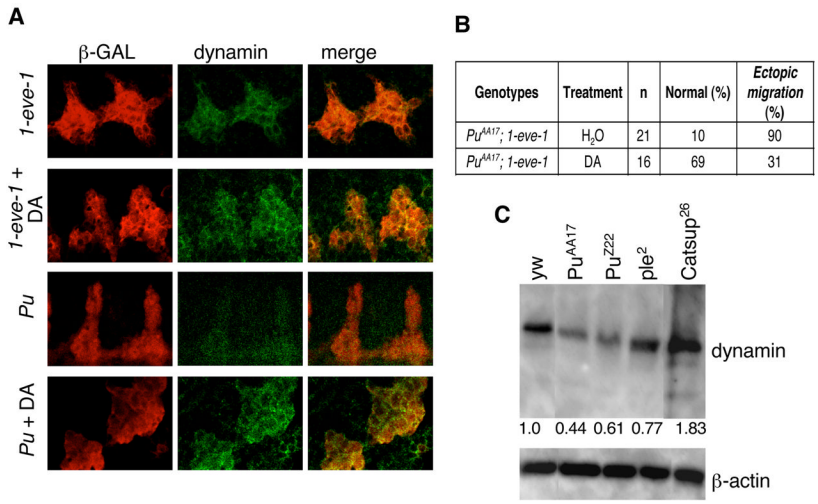

Genotypes	Treatment	n	Normal (%)	*Ectopic migration* (%)
Pu^{AA17}; 1-eve-1	H_2O	21	10	90
Pu^{AA17}; 1-eve-1	DA	16	69	31

Fig. 7.

Dynamin level is regulated by DA synthesis pathway components in the trachea. (A) *Drosophila* embryos of the genotypes *1-eve-1* (representing wild-type) or *Pu^{AA17}; 1-eve-1* (*Pu*) were double stained for β-Gal and dynamin. *1-eve-1* and *Pu* mutant embryos were treated with either H_2O or DA. Anterior is to the left and dorsal side is up. Images are zoomed-in view of 2 tracheal subunits. In untreated wild-type (*1-eve-1*) trachea, dynamin is enriched at the cell peripheries. DA treatment (*1-eve-1* + DA) slightly increased peripheral localization of dynamin in wild-type in both tracheal and neighboring cells. In the *Pu* mutant, dynamin level is reduced. DA treatment (*Pu* + DA) restored the level of dynamin. (B) *Pu^{AA17}; 1-eve-1* embryos were treated with either H_2O or DA (DA). Tracheal phenotypes were examined by staining for β-Gal. DA treatment rescued the *Pu* phenotype. (C) Total embryonic protein extracts from the indicated strains were Western-blotted for Shi/dynamin and reprobed for β-actin. Numbers under the protein lanes are the relative levels of dynamin normalized to the β-actin controls.

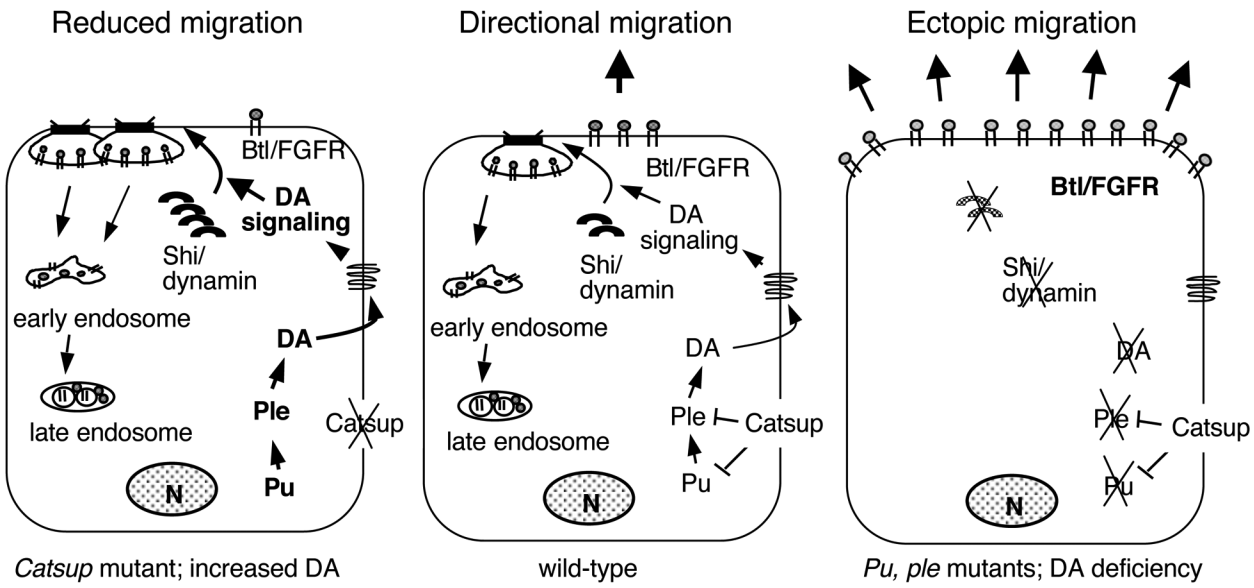

Fig. 8.

A model for the action of DA synthesis pathway genes. In wild-type cells (middle), the surface level of Btl/FGFR is modulated by endocytosis via the action of Shi/dynamin, while the stability of Shi/dynamin is regulated by DA, presumably through a DA-receptor mediated signaling event. In *Pu* or *ple* mutants (right), or when DA synthesis is blocked by 3-IT, Shi/dynamin level is reduced, resulting in over-accumulation of Btl/FGFR and ectopic migration. In *Catsup* mutants, or in the presence of exogenously added DA, the level of Shi/dynamin is increased, resulting in down-regulation of surface Btl/FGFR and reduced migration.

Table 1

Genetic interactions between DA synthesis and Btl endocytosis pathway genes.

Genotypes	n	% Normal	% Ectopic migration phenotype[a]		% Lack-of-migration phenotype[a]	
			moderate	severe	moderate	severe
Pu^{AA17}/+; 1-eve-1/+	24	16	71	13	0	0
awd^{J2A4}, 1-eve-1/+	26	19	69	12	0	0
shi^{2}/+ or Y; 1-eve-1/+	21	10	66	24	0	0
Pu^{AA17}/+; 1-eve-1/awd^{J2A4}, 1-eve-1	19	0	53	47	0	0
shi^{2}/+ or Y; Pu^{AA17}/+; 1-eve-1/+	17	0	53	47	0	0
btl^{H82D3}, 1-eve-1/+	25	16	0	0	60	24
Catsup^{26}/+; 1-eve-1/+	21	33	0	0	67	0
Catsup^{26}/+; 1-eve-1/btl^{H82D3}, 1-eve-1	18	0	0	0	55	45
Pu^{AA17}/+; 1-eve-1/btl^{H82D3}, 1-eve-1	22	41	46	0	13	0
Catsup^{26}/+; 1-eve-1/awd^{J2A4}, 1-eve-1	17	35	36	5	24	0
Pu^{Z22}/+; 1-eve-1/+	21	33	57	10	0	0
Pu^{Z22}/+; 1-eve-1/awd^{J2A4}, 1-eve-1	15	0	46	54	0	0
shi^{2}/+ or Y; Pu^{Z22}/+; 1-eve-1/+	16	0	44	56	0	0
Pu^{Z22}/+; 1-eve-1/btl^{H82D3}, 1-eve-1	20	35	35	5	25	0
Catsup^{26}/Pu^{AA17}	21	57	38	0	5	0
Catsup^{26}/Pu^{Z22}	19	74	26	0	0	0

[a] As defined in Figures 2 and S1. Moderate phenotype is defined as identifiable defects in tubule structures while the overall tubular network is intact. Severe phenotype is defined as lack of overall tracheal network due to disruption of organized tubule movement (ectopic migration) or severe blockade of migration.